HHS Public Access

Author manuscript

J Autoimmun. Author manuscript; available in PMC 2016 June 01.

Published in final edited form as:

J Autoimmun. 2015 June ; 60: 40–50. doi:10.1016/j.jaut.2015.03.005.

TNF-like weak inducer of apoptosis promotes blood brain barrier disruption and increases neuronal cell death in MRL/lpr mice

Jing Wen[a], **Jessica Doerner**[a], **Karen Weidenheim**[b], **Yumin Xia**[a], **Ariel Stock**[a], **Jennifer S. Michaelson**[c], **Kuti Baruch**[d], **Aleksandra Deczkowska**[d], **Maria Gulinello**[e], **Michal Schwartz**[d], **Linda C. Burkly**[f], and **Chaim Putterman**[a,g]

[a]Department of Microbiology and Immunology, Albert Einstein College of Medicine, Bronx, NY, USA, 10461

[b]Department of Neuropathology, Albert Einstein College of Medicine, Bronx, NY, USA, 10461

[c]Jounce Therapeutics, Cambridge, MA, USA, 02138

[d]Department of Neurobiology, Weizmann Institute of Science, Rehovot, Israel, 7610001

[e]Department of Neuroscience, Albert Einstein College of Medicine, Bronx, NY, USA, 10461

[f]Department of Immunology, Biogen Idec, Cambridge, MA, USA, 02142

[g]Division of Rheumatology and Department of Microbiology and Immunology, Albert Einstein College of Medicine, Bronx, NY, USA, 10461

Abstract

Neuropsychiatric disease is one of the most common manifestations of human systemic lupus erythematosus, but the mechanisms remain poorly understood. In human brain microvascular endothelial cells in vitro, TNF-like weak inducer of apoptosis (TWEAK) decreases tight junction ZO-1 expression and increases the permeability of monolayer cell cultures. Furthermore, knockout (KO) of the TWEAK receptor, Fn14, in the MRL/lpr lupus mouse strain markedly attenuates neuropsychiatric disease, as demonstrated by significant reductions in depressive-like behavior and improved cognitive function. The purpose of the present study was to determine the mechanisms by which TWEAK signaling is instrumental in the pathogenesis of neuropsychiatric lupus (NPSLE). Evaluating brain sections of MRL/lpr Fn14WT and Fn14KO mice, we found that Fn14KO mice displayed significantly decreased cellular infiltrates in the choroid plexus. To evaluate the integrity of the blood brain barrier (BBB) in MRL/lpr mice, Western blot for fibronectin, qPCR for iNOS, and immunohistochemical staining for VCAM-1/ICAM-1 were

Address Correspondence to: Chaim Putterman, MD, Division of Rheumatology, Albert Einstein College of Medicine, F701N, 1300 Morris Park Ave., Bronx, NY 10461, Tel. 718-430-4266, chaim.putterman@einstein.yu.edu.

Disclosure

Linda Burkly is a full time employee and stockholder of Biogen Idec. These studies were supported by research grants from Biogen Idec and the National Institutes of Health (DK090319 and AR065594) to C. Putterman.

performed. We found preserved BBB permeability in MRL/lpr Fn14KO mice, attributable to reduced brain expression of VCAM-1/ICAM-1 and iNOS. Additionally, administration of Fc-TWEAK intravenously directly increased the leakage of a tracer (dextran-FITC) into brain tissue. Furthermore, MRL/lpr Fn14KO mice displayed reduced antibody (IgG) and complement (C3, C6, and C4a) deposition in the brain. Finally, we found that MRL/lpr Fn14KO mice manifested reduced neuron degeneration and hippocampal gliosis. Our studies indicate that TWEAK/Fn14 interactions play an important role in the pathogenesis of NPSLE by increasing the accumulation of inflammatory cells in the choroid plexus, disrupting BBB integrity, and increasing neuronal damage, suggesting a novel target for therapy in this disease.

Keywords

1. Introduction

Systemic lupus erythematosus (SLE) is an autoimmune disease characterized by multi-organ damage, frequently involving the skin, kidney, and the brain. Central nervous system (CNS) involvement in lupus, or neuropsychiatric lupus (NPSLE), occurs in up to 40% of SLE patients. Patients with NPSLE can manifest a wide variety of neurological and psychiatric features, ranging from focal to diffuse presentations [1, 2]. Focal disorders include seizure activity and cerebrovascular events, which are often related to anti-phospholipid antibodies (aPL) [3], and vasculopathy [3, 4]. Diffuse manifestations, including cognitive impairment and mood disorders, are associated with inflammation [2, 3]. The most common manifestations of NPSLE are headache, mood disorders, and cognitive dysfunction, which significantly impair the quality of life and impact the prognosis of affected patients [5].

The mechanisms underlying NPSLE are not yet fully understood. Nevertheless, vascular abnormalities, autoantibodies, and inflammatory mediators are hypothesized as primary contributing factors [4]. Other studies have suggested a role for blood brain barrier (BBB) disruption [1, 6–8] and neuronal damage [9–13] in the pathogenesis of NPSLE. Currently, there is no specific or targeted therapies for NPSLE; most patients receive symptomatic therapy and/or various immunosuppressive agents [4].

The cytokine TNF-like weak inducer of apoptosis (TWEAK) is a TNF superfamily member that binds to Fn14, its sole known signaling receptor [14, 15]. Fn14 is normally expressed at relatively low levels in healthy tissue. In the brain, Fn14 is found in endothelial cells, astrocytes, neurons, and microglia at baseline, with a further increase in expression following exposure to various inflammatory stimuli [16]. Among the main effects induced by TWEAK and Fn14 interactions are inflammation, and cell death or cell proliferation depending on the particular cell type and cytokine context [17]. TWEAK/Fn14 signaling was found to contribute to the pathogenesis of an ischemic stroke model [18]. Additionally, in the experimental autoimmune encephalomyelitis (EAE) model of multiple sclerosis, blocking TWEAK/Fn14 interactions reduced immune cell infiltration into the CNS and the severity of disease [19].

The MRL/lpr strain is a well-established murine model for the study of NPSLE [20]. One major advantage of this model is that the neurologic manifestations are quite analogous to those present in human lupus patients, including early onset of disease [20]. In a recent study we found that TWEAK/Fn14 signaling is instrumental in the pathogenesis of murine NPSLE [21]; Fn14 deficiency attenuates NPSLE in MRL/lpr mice, as Fn14KO mice display significantly less depressive-like behavior and improved cognitive function [21].

Our aim in the current study was to elucidate the mechanism(s) by which TWEAK signaling is instrumental in the pathogenesis of NPSLE. We focused the investigation on the mechanisms for BBB disruption and neuronal damage, which are regarded as the key pathologic features in the MRL/lpr NPSLE model.

2. Material and methods

2.1. Mice

The detailed approach for generating 129 Fn14KO mice was described previously [20]. MRL/lpr Fn14KO mice were created by backcrossing 129 Fn14KO mice for 9 generations onto the MRL/lpr strain. Female MRL/lpr Fn14KO mice (Biogen Idec, Cambridge, MA) and MRL/lpr Fn14WT littermates derived from these crosses were used in this study in separate cohorts of 15 weeks and 20 weeks of age. Control age and gender matched MRL/MPJ (MPJ) mice were obtained from the Jackson Laboratory (Bar Harbor, ME). For Fc-TWEAK injection experiments, female MRL/lpr mice were purchased from Jackson Laboratory. The animals were handled according to the approved IACUC protocol #20140606 at the Albert Einstein College of Medicine.

2.2 Brain histology

Following extensive perfusion with cold PBS, the brain was divided into right and left hemispheres. The right brain hemisphere was used for sagittal paraffin sections. Part of the left brain hemisphere including the hippocampus was used for coronal frozen sections, and the remaining left hemispheric brain tissue was snap-frozen for preparation of brain lysates. Frozen cryostat sections (8 μm thick) were prepared for Fluoro Jade C staining. All other stainings were performed on paraffin-embedded sagittal sections (5 μm thick). For hematoxylin and eosin staining, two sections from each mouse were used to evaluate the cellular infiltration in the brain. The highest scores for each slide were used for the determination of lesion severity. For all other stains, one section from each mouse was analyzed. The histology slides were evaluated by 2 independent examiners.

2.3 Hematoxylin and eosin staining

Hematoxylin and eosin (H&E) staining was done by the histopathology core facility at the Albert Einstein College of Medicine. Briefly, 5 μm sagittal brain sections were mounted on Superfrost plus glass slides (Fisher Scientific); 2 sections per brain, 50 μm apart, were collected for evaluation. Slides were stained with H&E and evaluated by a veterinary pathologist. Infiltrates were scored on a scale of 0–4: 0=no lesions; 1=minimal; 2=mild; 3=moderate; and 4=severe.

2.4 Immunohistochemistry and immunofluorescence

For immunohistochemical staining of CD3, VCAM-1/ICAM-1, and B220, sections were incubated with the following primary antibodies: rat anti-human CD3 which reacts with mouse CD3 (Serotec, Raleigh, NC), rat anti-mouse VCAM-1 (Santa Cruz, Dallas, TX), rat anti-mouse ICAM-1 (Abcam, Cambridge, MA), and rat anti-mouse CD45R/B220 (BD Pharmingen, San Jose, CA), respectively, followed by a biotinylated secondary antibody (Jackson ImmunoResearch, West Grove, PA). For Ki-67 and Iba-1 staining, sections were individually incubated with rabbit anti-mouse Ki-67 (Vector Labs, Burlingame, CA) and rabbit anti-mouse Iba-1 (WAKO, Richmond, VA), followed by the DakoCytomation Envision+Dual Link System-HRP kit (Dako, Carpentaria, CA). For immunofluorescence staining, sections were incubated with rabbit anti-mouse glial fibrillary acidic protein (GFAP) (Millipore, Billerica, MA), followed by goat anti-rabbit IgG Alexa Fluor 594 (Jackson ImmunoResearch).

2.5 Evaluation of BBB permeability after Fc-TWEAK injection in vivo

To evaluate BBB permeability in vivo in response to TWEAK, MRL/lpr Fn14WT and Fn14KO mice were injected with mouse Fc-TWEAK [21]. In the first experiment, MRL/lpr mice (Jackson Laboratories) at 12 weeks of age were injected intravenously with 75 μg of Fc-TWEAK or the P1.17 murine IgG2a isotype control twice a week, for a total of eight injections. In the second experiment, 12 week old MRL/lpr Fn14WT and Fn14KO mice (Biogen Idec) were injected intravenously with 75 μg of Fc-TWEAK twice a week, for a total of eight injections. For both experiments, 24 hours after the last Fc-TWEAK injection, mice were injected with 10 mg dextran-FITC (150 KDa, Sigma, Northbrook, IL) via the tail vein as a tracer for BBB leakage. One hour later, mice were perfused and sacrificed. Brains were homogenized in PBS and centrifuged at 14,000 rpm for 10 minutes. After the first centrifugation, supernatant was separated from the pellets and methanol was added in a ratio of 2:1 (methanol:supernatant). This mixture was again centrifuged at 14,000 rpm for 10 minutes. After a second centrifugation the supernatant was collected, and the fluorescence in the supernatant measured at 485/535 nm.

2.6 Real-time qPCR

Cerebral cortexes were dissected from the brains of MRL/lpr Fn14WT and Fn14KO mice at 20 weeks of age. RNA samples were prepared by the RNeasy mini kit (Qiagen, Valencia, CA). cDNA synthesis was carried out using SuperScript III First-Strand Synthesis (Invitrogen, Carlsbad, CA). Real-time qPCR was performed in triplicate. Gene expression was normalized to GAPDH. Fold changes were calculated in reference to MRL/lpr Fn14KO mice, whose mean value was set at 1.

2.7 Fluoro Jade C and TUNEL staining

Fluoro Jade C staining was carried out as described previously [22]. Briefly, frozen sections were pretreated with 0.06% potassium permanganate, and then incubated with 0.001% Fluoro Jade C dye (Millipore, PA) in 0.1% acetic acid solution (pH 3.5). For TUNEL staining, an in-situ cell death detection (Fluroscein) kit (Roche, PA) was used. Slides were

examined under a fluorescence microscope (Zeiss AxioObserver CLEM) and the number of Fluoro Jade C or TUNEL positive cells was counted in each section.

2.8 Caspase-3 activity assay

Tissue caspase-3 activity was analyzed using the caspase-3 DEVD-R110 Fluorometric HTS assay kit and according to the manufacturer's instructions (Biotium, Hayward, CA). Briefly, 70 μg of brain lysates were incubated with the (Ac-DEVD)2-R110 substrate for an hour. Cleavage of the (Ac-DEVD)2-R110 substrate by activated caspase-3 leads to the release of a fluorescent dye (R110), which is then measured at 485/535 nm. Brain lysates from MRL/lpr Fn14WT mice incubated with Ac-DEVO-CHO, a caspase-3 inhibitor, served as the negative control.

2.9 Western blot

Brain tissues were lysed in 1 mL RIPA buffer (Cell Signaling, Danvers, MA) with 1 X protease cocktail inhibitor and 1 mM EDTA (Thermo Scientific Pierce, Rockford, IL). Lysates were loaded in NuPAGE Novex 10% Bis-Tris Gels (Invitrogen) and transferred to a PVDF membrane. The membrane was then separately incubated with the primary antibodies rabbit anti-mouse fibronectin (Abcam, Cambridge, MA), rabbit anti-mouse C6 (Santa Cruz), goat anti-mouse C3 (MP Biomedicals, Santa Ana, CA), and rabbit anti-mouse β-actin (Cell Signaling), followed by the corresponding secondary antibody and chemiluminescence substrate (Thermo Scientific Pierce). For IgG detection, the membrane was directly incubated with goat-anti mouse IgG-HRP (Southern Biotech, Birmingham, AL). Quantitation of band densities was performed by Image J, and expressed relative to β-actin.

2.10 Object placement (OP) test

Object placement is a cognitive function test used to evaluate spatial memory [23]. Generally, similar to humans, mice have an innate preference to explore novel rather than familiar locations [24]. Briefly, mice were first familiarized with two identical objects in two different locations over 5 minutes. After a 20 minute retention interval outside the arena during which one object was left in its original place while the other object was moved to a new location, the mice were retested for their exploration preference. The preference score (%) of OP was calculated as [exploration time in the novel place]/[exploration time in both places] × 100. The scoring was done manually in a blinded manner.

2.11 Statistical analysis

Graphpad Prism 6 software was employed for statistical analysis. Mean ±standard error of the mean (SEM) was used to represent the data in each graph. Differences between two groups were analyzed by an unpaired t test (two tailed). The Chi-square test was employed to compare the incidence of cellular infiltration in the choroid plexus between the experimental groups. P values of less than 0.05 were considered significant.

3. Results

3.1 Fn14 deficiency decreases the incidence and severity of cellular infiltration into the brain of lupus mice

To investigate whether the neurobehavioral differences in emotionality and cognition that were observed between MRL/lpr Fn14WT and Fn14KO mice correlated with histopathological abnormalities, brain sections at 15 and 20 weeks of age were examined. At 15 weeks of age, MRL/lpr Fn14WT mice displayed minimal cellular infiltration, with no significant differences between the MRL/lpr Fn14WT and Fn14KO mice (data not shown). In contrast, at 20 weeks of age, MRL/lpr Fn14WT mice exhibited significant cellular infiltration, predominantly localized to the subependymal regions and choroid plexus of the third and fourth ventricles with few infiltrates observed also in the brain parenchyma (Figure 1A). Ten MRL/lpr Fn14WT brains were evaluated; of these, 9 had lymphocytic subependymal and choroid plexus infiltrates in the third ventricle (Figure 1B). Inflammation in the region of the fourth ventricle was present as well, with 5/10 MRL/lpr Fn14WT mice showing lymphocytic infiltrates (Figure 1B). In addition, 5/10 MRL/lpr Fn14WT mice had minimal-mild but appreciable choroid plexus cellular hypertrophy, which was concomitant with inflammation (data not shown). In contrast, MRL/lpr Fn14KO mice had a lower incidence of, and less severe, inflammatory infiltrates in the brain, as compared to MRL/lpr Fn14WT mice. Of 8 MRL/lpr Fn14KO mice, only 3 had lymphocytic infiltrates into the choroid plexus associated with the third ventricle, with no inflammation present around the fourth ventricle in any mouse (Figure 1B). The total infiltration score (the sum of infiltration scores in the third or fourth ventricle) (Figure 1C) indicates a significant reduction in the severity of the infiltration in MRL/lpr Fn14KO mice. The control MRL/MPJ mice had no inflammatory infiltrates in the brain.

Immunohistochemical staining for T cells (CD3), macrophages/microglia (Iba-1), and B cells (B220) was performed to determine the composition of the cellular infiltrates. We found that T cells and Iba-1^+ cells (which were morphologically macrophages) were the predominant populations present in the choroid plexus infiltrates (Figure 2A). Notably, MRL/lpr Fn14KO mice showed significantly reduced infiltration of T cells, macrophages, and B cells (Figure 2B).

3.2 The role of TWEAK signaling in breakdown of the BBB in MRL/lpr mice

Recent studies suggest that BBB impairment is a key physiopathological feature in NPSLE [1, 7, 8, 22]. Moreover, we had previously reported that MRL/lpr Fn14WT mice have increased albumin and IgG concentrations in the CSF [21]. Increased BBB permeability is associated with the accumulation of extracellular matrix components such as fibronectin and laminin around blood vessels, through extravasation from the plasma and deposition in brain tissue [22]. The following series of experiments was performed to confirm that activation of the TWEAK/Fn14 axis modulates changes in BBB permeability in MRL/lpr mice, and to understand the mechanism. First, Western blotting for fibronectin was performed. We found that fibronectin deposition was significantly reduced in the brain of MRL/lpr Fn14KO mice as compared to MRL/lpr Fn14WT at 20 weeks of age (Figure 3A), consistent with improved BBB integrity.

Adhesion molecules play an important role in BBB disruption by facilitating immune cell transmigration, thereby promoting further inflammation in the brain [23]. Previously, we had found that TWEAK upregulates VCAM-1 and ICAM-1 expression in brain microvascular endothelial cells in vitro [24]. To address a possible role for altered adhesion molecule expression in MRL/lpr Fn14WT mice, we investigated brain VCAM-1 and ICAM-1 expression in vivo. Immunohistochemical staining revealed that VCAM-1 and ICAM-1 expression in endothelial cells was prominent in periventricular areas (Figure 3B). In contrast, MRL/lpr Fn14KO mice showed significantly decreased VCAM-1 staining, and exhibited similarly diminished ICAM-1 expression (Figure 3B).

Inducible nitric oxide synthetase (iNOS) is an important inflammatory mediator of BBB breakdown. Most cytokines that can modulate BBB properties, such as TNF, IL-1β, IFN-γ, and IL-6, are potent iNOS generators [25]. Additionally, Alexander et al reported abundant iNOS production in brains of MRL/lpr mice [26]. To further investigate whether TWEAK/Fn14 interactions are related to iNOS production in NPSLE, iNOS expression in cortical samples of MRL/lpr Fn14WT and Fn14KO mice was measured by qRT-PCR. As seen in Figure 3C, MRL/lpr Fn14KO mice showed significantly decreased levels of iNOS expression in the cortex.

To establish if the increase in BBB permeability in murine lupus can be directly triggered through TWEAK/Fn14 signaling, Fc-TWEAK was injected intravenously to MRL/lpr mice. We found that MRL/lpr mice treated with Fc-TWEAK had increased brain extravasation of intravenously administered dextran-FITC as compared to control IgG treated mice (Figure 3D). Confirming that this effect is indeed mediated by Fn14 and not a contaminant, Fc-TWEAK treated MRL/lpr Fn14WT mice displayed a significant increase in the fluorescence signal found in the brain as compared to Fc-TWEAK treated MRL/lpr Fn14KO mice (Figure 3E). Injection of Fc-TWEAK in MRL/lpr Fn14WT mice did not significantly increase Fn14 expression (data not shown). These studies convincingly demonstrate that TWEAK/Fn14 signaling can induce BBB breakdown in the MRL/lpr strain.

Once the BBB is breached, inflammatory mediators may reach the brain parenchyma and activate microglia [27]. In order to evaluate microglial activation in murine lupus brain and study whether Fn14 deficiency may modulate the state of microglial activation, Iba-1 staining was employed. Iba-1 staining was analyzed in cortex, hippocampus, and periventricular areas, since the cortex and hippocampus are related to emotion and cognitive function [28]. However, no significant differences were seen in microglial staining between MRL/lpr Fn14WT and KO mice in all 3 anatomical locations (Figure 4A–D). Nevertheless, we observed that in MRL/MPJ mice the most dominant microglial morphology was a highly ramified phenotype, while MRL/lpr Fn14WT and Fn14KO mice exhibited a higher percentage of less ramified and ameboid microglia (Figure 4A).

3.3 Antibody deposition and complement activation are decreased in brains of MRL/lpr Fn14KO mice

One characteristic feature of lupus is the presence of high titers of serum autoantibodies, many of which are potentially neurotoxic. In the setting of a compromised BBB, these autoantibodies from the periphery can bypass the BBB and deposit in the brain. To establish

that a breached BBB in MRL/lpr Fn14WT mice is associated with an increase in brain deposited IgG, Western blotting of brain lysates was performed. Previously, we reported no differences in the concentration of serum IgG autoantibodies and total IgG between MRL/lpr Fn14WT and Fn14KO mice [21]. Nevertheless, MRL/lpr Fn14KO mice exhibited decreased brain IgG deposition (Figure 5A, B), which is also supportive of better preserved BBB integrity in this strain.

Antibody deposition and immune complex formation are potent activators of the classical pathway of complement activation, which is initiated by the activation of C1s leading to the cleavage of C4 into C4a and C4b. The binding of C4b and C2b forms C3 convertase which cleaves C3, followed by the assembly of the C5b, C6, C7, C8 and C9 membrane attack complex (MAC), resulting in cell death. Consistent with the decreased brain deposition of IgG seen by Western blot, C3 (Figure 5A, 5B), C6 (Figure 5A, 5B, 5C), and C4a (Figure 5D) were significantly downregulated in the brains of MRL/lpr Fn14KO mice.

3.4 Fn14 deficiency reduces brain apoptosis

One of the most well characterized effects of TWEAK/Fn14 interactions is the induction of apoptosis, which is a predominant feature in the brain of lupus mice [9, 10, 26]. To investigate whether Fn14 deficiency has any effects on brain apoptosis, TUNEL staining was performed at 15 and 20 weeks of age. At 15 weeks of age, very few TUNEL positive cells were observed in the brain of MRL/lpr Fn14WT mice (data not shown). However, at 20 weeks of age, MRL/lpr Fn14WT mice displayed a significant increase in TUNEL positive cells, predominantly within the choroid plexus (Figure 6A), and to a lesser degree in the periventricular areas. Quantification of the total number of TUNEL positive cells confirmed that Fn14 deficiency reduced apoptosis in the brain of MRL/lpr mice (Figure 6B). Consistent with the results of TUNEL staining, decreased brain caspase-3 activity at 20 weeks of age was observed in MRL/lpr Fn14KO as compared to MRL/lpr Fn14WT mice, further supporting that Fn14 deficiency was associated with attenuated brain apoptosis (Figure 6C).

TUNEL staining detects apoptosis in all cell types, while Fluoro Jade C, which specifically stains apoptotic and necrotic neurons, is used to selectively evaluate neuronal degeneration. At 15 weeks of age, significantly more Fluoro Jade C positive degenerating neurons, predominantly in the cortex, were present in MRL/lpr Fn14WT as compared to Fn14KO mice (Figure 6D, 6E). A few Fluoro Jade C positive neurons were seen in the hippocampus at this time point, with no significant differences between MRL/lpr Fn14WT and Fn14KO mice. However, neuronal degeneration increased with age. At 20 weeks of age, an increased number of degenerating neurons were observed both in MRL/lpr Fn14WT and Fn14KO mice with no significant differences between the strains (data not shown).

Next, in order to investigate whether the increased neuron degeneration in the brains of MRL/lpr Fn14WT mice at 15 weeks of age was due to impaired neurogenesis, Ki-67 staining was performed. The major areas that neurogenesis occurs in murine NPSLE are the hippocampus, rosal migratory stream, and subventricular zone [29]. We found that at 15 weeks of age, there were no significant differences in neurogenesis in these areas among MRL/lpr Fn14WT, MRL/lpr Fn14KO, and MRL/MPJ mice (data not shown).

3.5 Fn14 deficiency diminishes hippocampal gliosis

Fn14 deficient MRL/lpr mice have improved cognitive function, especially spatial memory [21], which is associated with the integrity of hippocampus [30]. Alexander et al previously reported that MRL/lpr mice demonstrated increased hippocampal gliosis (i.e. astrocyte activation/proliferation) [31]. To investigate whether Fn14 deficiency diminishes hippocampal gliosis, GFAP staining was performed. GFAP staining indicated that MRL/lpr Fn14WT mice displayed intense astrocyte activation in the hippocampus, while MRL/lpr Fn14KO mice showed reduced levels of hippocampal gliosis (Figure 7A, 7B). To address a possible pathogenic link between hippocampal damage and spatial memory, we compared the scores of hippocampal gliosis to the preference scores in the object placement test in individual mice. Interestingly, the correlation analysis indicated that abnormal spatial memory (lower OP preference scores) significantly correlated with increased hippocampal gliosis (Figure 7C).

4. Discussion

The MRL/lpr strain is one of the most widely used murine models to study NPSLE. Previously, we reported that Fn14 deficiency ameliorated NPSLE in this strain, as demonstrated by diminished depressive-like behavior and preserved cognitive function [21]. However, the mechanisms that contribute to the attenuation of the neuropsychiatric phenotype in MRL/lpr Fn14KO mice needed to be clarified. In this study, we found that prevention of TWEAK/Fn14 signaling in MRL/lpr Fn14KO mice decreased the accumulation of choroid plexus infiltrates, reduced expression of VCAM-1/ICAM-1 and iNOS, and decreased brain apoptosis and neuronal death.

One of the most prominent pathological features found in the brains of MRL/lpr mice is immune cell infiltration. Consistent with previous reports [32], we found that immune cell infiltration began in the choroid plexus at around 15 weeks of age and became pronounced by 20 weeks of age. Since there is no BBB but rather a blood-CSF barrier in the choroid plexus [33], local or systemic mediators from the periphery may promote CNS injury by promoting inflammation and/or initiating immune cell entry into the brain through the choroid plexus.

We observed that the brain cellular infiltrates present in MRL/lpr Fn14WT mice were primarily composed of T cells, macrophages, and to a lesser extent B cells. The T cell phenotype of brain infiltrating cells in murine NPSLE has been previously characterized as $CD4^+$ T cells [32] or $CD4^-$ $CD8^-$ double negative T cells [34]. Since Fn14 is inducible in epithelial cells [35] and TWEAK is increased in NPSLE in the CSF [36], TWEAK may stimulate choroid plexus epithelial cells to secrete chemotactic factors and increase adhesion molecule expression, which can contribute to the recruitment of immune cells across the blood-CSF barrier [40].

Disruption of the BBB is associated with several non-inflammatory and inflammatory diseases of the CNS. Yepes et al. reported that TWEAK/Fn14 interactions facilitated neutrophil transmigration and increased BBB permeability in an ischemic stroke model [37, 38]. Similarly, Marjaneh et al. suggested that blocking TWEAK/Fn14 interactions

attenuated the increase in BBB permeability in EAE [39]. In NPSLE patients, a compromised BBB is evidenced by the increased albumin quotient in the CSF and enhanced gadolinium leakage by MRI [40, 41]. Similarly, in the MRL/lpr mouse model, extravasation of IgG-Alexa Fluor 488 from the plasma into the brain parenchyma and increased fibronectin deposition reflect a disturbed BBB [1, 7, 8]. Our study confirms that Fn14 deficiency preserves BBB integrity in MRL/lpr mice. Additionally, we have conclusively shown here that activation of the TWEAK/Fn14 pathway can directly compromise BBB integrity in the MRL/lpr strain. The increased BBB permeability in Fn14-sufficient lupus mice may due to the decreased expression of tight junction protein ZO-1, upregulated expression of MCP-1, IL-6, and IL-8, and increased ICAM-1 and VCAM-1 expression, as these effects were induced by TWEAK in (non-MRL/lpr-derived) brain microvascular endothelial cells in an in vitro BBB model [24]. Thus, the effects of TWEAK on the BBB are not limited to autoimmune mice. Indeed, Polavarapu et al reported that direct administration of TWEAK into the striatum increased BBB permeability in C57/B6 mice [42].

We found here that VCAM-1 and ICAM-1 staining of endothelial cells was most intense in the periventricular area, where the BBB is most fragile [43]. T and B cells were also found in the periventricular areas, suggesting a breach of the BBB in this region. Endothelial dysfunction in the periventricular areas may result from the prominent inflammation in the choroid plexus, since these two sites are adjacent to each other.

Microglia play an important role in brain surveillance. With a compromised BBB the brain can be affected by a variety of inflammatory mediators, and thereby microglia can become activated. Although using F4/80 staining Ballok et al found more intense microglial activation in the cortex, hypothalamus, and cerebellum in MRL/lpr as compared to the control MRL/MPJ strain [44], our study did not find significant differences in microglial activation (as indicated by Iba-1 positivity) among MRL/lpr Fn14WT, MRL/lpr Fn14KO, and MRL/MPJ mice. Nevertheless, while highly ramified microglia regarded as resting or inactive [45] were prominent in MRL/MPJ mice, the less ramified and ameboid phenotype was relatively more abundant in the MRL/lpr strains. The detailed characterization of the specific M1 or M2 microglial phenotype may be helpful in further dissection of the role of microglial activation in this disease.

Autoantibodies play an important role in NPSLE. Kowal et al demonstrated that with a breached BBB, autoantibodies such as anti-NMDA receptor antibodies could reach the brain and bind to hippocampal neurons to induce neuronal death [46], leading to cognitive impairment. Additionally, injection of anti-ribosomal P antibodies into the brain induces olfactory dysfunction and depressive-like behavior [47]. Autoantibodies can directly deposit in the limbic/olfactory system including the piriform cortex, hippocampus, and cingulate cortex, which have been implicated in mood disorders and cognitive dysfunction [47, 48]. Local complement activation may further augment the inflammatory cascade, ultimately adding to global brain injury and dysfunction. In this study, we focused on complement components previously shown to play a role in the pathogenesis of autoimmune brain disease. C3, C4 and C6 have been implicated in EAE, a model for multiple sclerosis [49–51]. Moreover, C3 and C4 have been reported to be involved in the pathogenesis of NPSLE

[26, 52, 53]. The prerequisite for the entry of autoantibodies into the brain is a compromised BBB; here, we found that Fn14 deficient MRL/lpr mice exhibit less IgG and C3 deposition, which may be due to improved BBB integrity.

Apart from the disruption of the BBB, neuronal damage is another key feature in NPSLE. Consistent with previous studies [9, 10], we found that MRL/lpr mice displayed increased brain cell death, while in the current study we observed that Fn14 deficiency reduced the number of apoptotic cells and degenerating neurons. The differences in staining between Fluoro Jade C and TUNEL is likely due to the fact that TUNEL positivity is specifically a marker for late apoptosis and in all cell types, while Fluoro Jade C is more selective and targets neurons, both apoptotic and necrotic [9]. In vitro, TWEAK/Fn14 interactions induce neuronal death via the NF-kB signaling pathway [54, 55].

Another indicator of neuronal damage is astrocyte activation and proliferation, also known as gliosis. Upon activation, astrocytes can produce abundant inflammatory mediators that further injure the surrounding areas in the brain. In vitro, astrocytes upregulate IL-6 and IL-8 following TWEAK stimulation [56]. In our current study, we found that Fn14 deficiency ameliorated hippocampal gliosis in MRL/lpr mice. The hippocampus has a critical role in memory processes, especially in the establishment of spatial learning [57]. Our correlation analysis indicated that the reduced hippocampal gliosis scores in MRL/lpr Fn14KO mice might be responsible for the better preserved cognitive function in this strain.

5. Conclusions

In summary, we found that Fn14 deficiency reduced choroid plexus cellular infiltration, diminished VCAM/ICAM-1 and iNOS expression, and decreased brain cell death in lupus prone MRL/lpr mice. An important remaining question is whether TWEAK/Fn14 signaling in the CNS or in the periphery is the major contributor to NPSLE. The increased brain TWEAK levels reported previously can be coming from the circulation, or secreted locally by astrocytes and microglia. TWEAK/Fn14 interactions in the periphery may also upregulate circulating concentrations of neuroactive cytokines. Furthermore, high TWEAK levels can contribute to permeabilization of the blood-CSF and blood-brain barriers, which may further amplify the inflammatory cascade in the CNS. Although outside the scope of the present study, this question can be studied in the future using bone marrow chimera approaches or by generating of brain cell specific Fn14KO mouse strains. Nonetheless, our study points to several mechanisms by which TWEAK/Fn14 interactions may contribute to the pathogenesis of NPSLE, and provides additional support that this cytokine-receptor dyad is a potential new target for therapy.

Acknowledgments

We would like to thank Dr. Rani Sellers, the Director of the Histology and Comparative Pathology Facility at Albert Einstein College of Medicine, for her assistance in quantitating the brain cellular infiltrates.

References

1. Abbott NJ, Mendonca LL, Dolman DE. The blood-brain barrier in systemic lupus erythematosus. Lupus. 2003; 12:908–15. [PubMed: 14714910]

2. Bertsias GK, Boumpas DT. Pathogenesis, diagnosis and management of neuropsychiatric SLE manifestations. Nature Rev Rheumatol. 2010; 6:358–67. [PubMed: 20458332]
3. Hanly JG. Neuropsychiatric lupus. Curr Rheum Reports. 2001; 3:205–12.
4. Hanly JG. Diagnosis and management of neuropsychiatric SLE. Nature Rev Rheumatol. 2014; 10:338–47. [PubMed: 24514913]
5. Hanly JG, Urowitz MB, Sanchez-Guerrero J, Bae SC, Gordon C, Wallace DJ, et al. Neuropsychiatric events at the time of diagnosis of systemic lupus erythematosus: an international inception cohort study. Arthritis Rheum. 2007; 56:265–73. [PubMed: 17195230]
6. Stock AD, Wen J, Putterman C. Neuropsychiatric lupus, the blood brain barrier, and the TWEAK/Fn14 pathway. Front Immunol. 2013; 4:484. [PubMed: 24400009]
7. Jacob A, Hack B, Chen P, Quigg RJ, Alexander JJ. C5a/CD88 signaling alters blood-brain barrier integrity in lupus through nuclear factor-kappaB. J Neurochem. 2011; 119:1041–51. [PubMed: 21929539]
8. Jacob A, Hack B, Chiang E, Garcia JG, Quigg RJ, Alexander JJ. C5a alters blood-brain barrier integrity in experimental lupus. FASEB J. 2010; 24:1682–8. [PubMed: 20065106]
9. Ballok DA, Millward JM, Sakic B. Neurodegeneration in autoimmune MRL-lpr mice as revealed by Fluoro Jade B staining. Brain Res. 2003; 964:200–10. [PubMed: 12576180]
10. Sakic B, Maric I, Koeberle PD, Millward JM, Szechtman H, Maric D, et al. Increased TUNEL staining in brains of autoimmune Fas-deficient mice. J Neuroimmunol. 2000; 104:147–54. [PubMed: 10713354]
11. Sakic B, Szechtman H, Denburg JA, Gorny G, Kolb B, Whishaw IQ. Progressive atrophy of pyramidal neuron dendrites in autoimmune MRL-lpr mice. J Neuroimmunol. 1998; 87:162–70. [PubMed: 9670858]
12. Sakic B, Kolb B, Whishaw IQ, Gorny G, Szechtman H, Denburg JA. Immunosuppression prevents neuronal atrophy in lupus-prone mice: evidence for brain damage induced by autoimmune disease? J Neuroimmunol. 2000; 111:93–101. [PubMed: 11063826]
13. Ballok DA, Woulfe J, Sur M, Cyr M, Sakic B. Hippocampal damage in mouse and human forms of systemic autoimmune disease. Hippocampus. 2004; 14:649–61. [PubMed: 15301441]
14. Campbell S, Burkly LC, Gao HX, Berman JW, Su L, Browning B, et al. Proinflammatory effects of TWEAK/Fn14 interactions in glomerular mesangial cells. J Immunol. 2006; 176:1889–98. [PubMed: 16424220]
15. Michaelson JS, Wisniacki N, Burkly LC, Putterman C. Role of TWEAK in lupus nephritis: a bench-to-bedside review. J Autoimmunity. 2012; 39:130–42. [PubMed: 22727560]
16. Yepes M. TWEAK and the central nervous system. Mol Neurobiol. 2007; 35:255–65. [PubMed: 17917114]
17. Campbell S, Michaelson J, Burkly L, Putterman C. The role of TWEAK/Fn14 in the pathogenesis of inflammation and systemic autoimmunity. Front Biosci. 2004; 9:2273–84. [PubMed: 15353286]
18. Zhang X, Winkles JA, Gongora MC, Polavarapu R, Michaelson JS, Hahm K, et al. TWEAK-Fn14 pathway inhibition protects the integrity of the neurovascular unit during cerebral ischemia. J Cereb Blood Flow Metabol. 2007; 27:534–44.
19. Prinz-Hadad H, Mizrachi T, Irony-Tur-Sinai M, Prigozhina TB, Aronin A, Brenner T, et al. Amelioration of autoimmune neuroinflammation by the fusion molecule Fn14. TRAIL J Neuroinflammation. 2013; 10:36.
20. Gulinello M, Putterman C. The MRL/lpr mouse strain as a model for neuropsychiatric systemic lupus erythematosus. J Biomed Biotechnol. 2011; 2011:207504. [PubMed: 21331367]
21. Wen J, Xia Y, Stock A, Michaelson JS, Burkly LC, Gulinello M, et al. Neuropsychiatric disease in murine lupus is dependent on the TWEAK/Fn14 pathway. J Autoimmunity. 2013; 43:44–54. [PubMed: 23578591]
22. Alexander JJ, Jacob A, Vezina P, Sekine H, Gilkeson GS, Quigg RJ. Absence of functional alternative complement pathway alleviates lupus cerebritis. Eur J Immunol. 2007; 37:1691–701. [PubMed: 17523212]
23. Whalen MJ, Carlos TM, Kochanek PM, Heineman S. Blood-brain barrier permeability, neutrophil accumulation and vascular adhesion molecule expression after controlled cortical impact in rats: a preliminary study. Acta Neurochirurgica (Supplement). 1998; 71:212–4. [PubMed: 9779187]

24. Stephan D, Sbai O, Wen J, Couraud PO, Putterman C, Khrestchatisky M, et al. TWEAK/Fn14 pathway modulates properties of a human microvascular endothelial cell model of blood brain barrier. J Neuroinflammation. 2013; 10:9. [PubMed: 23320797]
25. Mayhan WG. Nitric oxide donor-induced increase in permeability of the blood-brain barrier. Brain Res. 2000; 866:101–8. [PubMed: 10825485]
26. Alexander JJ, Jacob A, Bao L, Macdonald RL, Quigg RJ. Complement-dependent apoptosis and inflammatory gene changes in murine lupus cerebritis. J Immunol. 2005; 175:8312–9. [PubMed: 16339572]
27. Benarroch EE. Microglia: Multiple roles in surveillance, circuit shaping, and response to injury. Neurology. 2013; 81:1079–88. [PubMed: 23946308]
28. Vertes RP. Interactions among the medial prefrontal cortex, hippocampus and midline thalamus in emotional and cognitive processing in the rat. Neuroscience. 2006; 142:1–20. [PubMed: 16887277]
29. Stanojcic M, Burstyn-Cohen T, Nashi N, Lemke G, Sakic B. Disturbed distribution of proliferative brain cells during lupus-like disease. Brain Behav Immun. 2009; 23:1003–13. [PubMed: 19501646]
30. Broadbent NJ, Gaskin S, Squire LR, Clark RE. Object recognition memory and the rodent hippocampus. Learn Mem. 2010; 17:5–11. [PubMed: 20028732]
31. Jacob A, Bao L, Brorson J, Quigg RJ, Alexander JJ. C3aR inhibition reduces neurodegeneration in experimental lupus. Lupus. 2010; 19:73–82. [PubMed: 19900981]
32. Vogelweid CM, Johnson GC, Besch-Williford CL, Basler J, Walker SE. Inflammatory central nervous system disease in lupus-prone MRL/lpr mice: comparative histologic and immunohistochemical findings. J Neuroimmunol. 1991; 35:89–99. [PubMed: 1955574]
33. Segal MB. The choroid plexuses and the barriers between the blood and the cerebrospinal fluid. Cell Mol Neurobiol. 2000; 20:183–96. [PubMed: 10696509]
34. James WG, Hutchinson P, Bullard DC, Hickey MJ. Cerebral leucocyte infiltration in lupus-prone MRL/MpJ-fas lpr mice--roles of intercellular adhesion molecule-1 and P-selectin. Clin Exp Immunol. 2006; 144:299–308. [PubMed: 16634804]
35. Ebihara N, Nakayama M, Tokura T, Iwatsu M, Ushio H, Murakami A. Proinflammatory effect of TWEAK/Fn14 interaction in human retinal pigment epithelial cells. Curr Eye Res. 2009; 34:836–44. [PubMed: 19895311]
36. Trysberg EBLSL, Michaelson J, Putterman C. Cerebrospinal fluid (CSF) TWEAK: a novel biomarker for neuropsychiatric SLE? Arthritis Rheum. 2007; 56:S750.
37. Yepes M, Brown SA, Moore EG, Smith EP, Lawrence DA, Winkles JA. A soluble Fn14-Fc decoy receptor reduces infarct volume in a murine model of cerebral ischemia. Amer J Pathol. 2005; 166:511–20. [PubMed: 15681834]
38. Haile WB, Echeverry R, Wu J, Yepes M. The interaction between tumor necrosis factor-like weak inducer of apoptosis and its receptor fibroblast growth factor-inducible 14 promotes the recruitment of neutrophils into the ischemic brain. J Cereb Blood Flow Metabol. 2010; 30:1147–56.
39. Razmara M, Hilliard B, Ziarani AK, Murali R, Yellayi S, Ghazanfar M, et al. Fn14-TRAIL, a chimeric intercellular signal exchanger, attenuates experimental autoimmune encephalomyelitis. Amer J Pathol. 2009; 174:460–74. [PubMed: 19147815]
40. Winfield JB, Shaw M, Silverman LM, Eisenberg RA, Wilson HA 3rd, Koffler D. Intrathecal IgG synthesis and blood-brain barrier impairment in patients with systemic lupus erythematosus and central nervous system dysfunction. Amer J Med. 1983; 74:837–44. [PubMed: 6837607]
41. McLean BN, Miller D, Thompson EJ. Oligoclonal banding of IgG in CSF, blood-brain barrier function, and MRI findings in patients with sarcoidosis, systemic lupus erythematosus, and Behcet's disease involving the nervous system. J Neurol Neurosurg Psych. 1995; 58:548–54.
42. Polavarapu R, Gongora MC, Winkles JA, Yepes M. Tumor necrosis factor-like weak inducer of apoptosis increases the permeability of the neurovascular unit through nuclear factor-kappa B pathway activation. J Neurosci. 2005; 25:10094–100. [PubMed: 16267216]

43. Ueno M, Akiguchi I, Hosokawa M, Kotani H, Kanenishi K, Sakamoto H. Blood-brain barrier permeability in the periventricular areas of the normal mouse brain. Acta Neuropathologica. 2000; 99:385–92. [PubMed: 10787037]
44. Ballok DA, Ma X, Denburg JA, Arsenault L, Sakic B. Ibuprofen fails to prevent brain pathology in a model of neuropsychiatric lupus. J Rheum. 2006; 33:2199–213. [PubMed: 17086606]
45. Katsumoto A, Lu H, Miranda AS, Ransohoff RM. Ontogeny and functions of central nervous system macrophages. J Immunol. 2014; 193:2615–21. [PubMed: 25193935]
46. Kowal C, Degiorgio LA, Lee JY, Edgar MA, Huerta PT, Volpe BT, et al. Human lupus autoantibodies against NMDA receptors mediate cognitive impairment. Proc Natl Acad Sci USA. 2006; 103:19854–9. [PubMed: 17170137]
47. Katzav A, Solodeev I, Brodsky O, Chapman J, Pick CG, Blank M, et al. Induction of autoimmune depression in mice by anti-ribosomal P antibodies via the limbic system. Arthritis Rheum. 2007; 56:938–48. [PubMed: 17328071]
48. Kowal C, Diamond B. Aspects of CNS lupus: mouse models of anti-NMDA receptor antibody mediated reactivity. Methods Mol Biol. 2012; 900:181–206. [PubMed: 22933070]
49. Ingram G, Hakobyan S, Hirst CL, Harris CL, Loveless S, Mitchell JP, et al. Systemic complement profiling in multiple sclerosis as a biomarker of disease state. Multiple Sclerosis. 2012; 18:1401–11. [PubMed: 22354735]
50. Mead RJ, Singhrao SK, Neal JW, Lassmann H, Morgan BP. The membrane attack complex of complement causes severe demyelination associated with acute axonal injury. J Immunol. 2002; 168:458–65. [PubMed: 11751993]
51. Ingram G, Hakobyan S, Robertson NP, Morgan BP. Complement in multiple sclerosis: its role in disease and potential as a biomarker. Clin Exp Immunol. 2009; 155:128–39. [PubMed: 19040603]
52. Jongen PJ, Boerbooms AM, Lamers KJ, Raes BC, Vierwinden G. Diffuse CNS involvement in systemic lupus erythematosus: intrathecal synthesis of the 4th component of complement. Neurology. 1990; 40:1593–6. [PubMed: 2215952]
53. Karassa FB, Ioannidis JP, Touloumi G, Boki KA, Moutsopoulos HM. Risk factors for central nervous system involvement in systemic lupus erythematosus. QJM. 2000; 93:169–74. [PubMed: 10751236]
54. Haile WB, Echeverry R, Wu F, Guzman J, An J, Wu J, et al. Tumor necrosis factor-like weak inducer of apoptosis and fibroblast growth factor-inducible 14 mediate cerebral ischemia-induced poly(ADP-ribose) polymerase-1 activation and neuronal death. Neuroscience. 2010; 171:1256–64. [PubMed: 20955770]
55. Potrovita I, Zhang W, Burkly L, Hahm K, Lincecum J, Wang MZ, et al. Tumor necrosis factor-like weak inducer of apoptosis-induced neurodegeneration. J Neurosci. 2004; 24:8237–44. [PubMed: 15385607]
56. Saas P, Boucraut J, Walker PR, Quiquerez AL, Billot M, Desplat-Jego S, et al. TWEAK stimulation of astrocytes and the proinflammatory consequences. Glia. 2000; 32:102–7. [PubMed: 10975915]
57. Eichenbaum H. Hippocampus: cognitive processes and neural representations that underlie declarative memory. Neuron. 2004; 44:109–20. [PubMed: 15450164]

Highlights

1. The absence of Fn14 decreases inflammation in the choroid plexus of lupus mice.
2. Fn14 deficiency reduces brain expression of VCAM-1, ICAM-1, and iNOS in MRL/lpr.
3. Fc-TWEAK directly increases blood brain barrier permeability in lupus-prone mice.
4. Fn14 deficiency attenuates neuron degeneration and brain cell apoptosis.

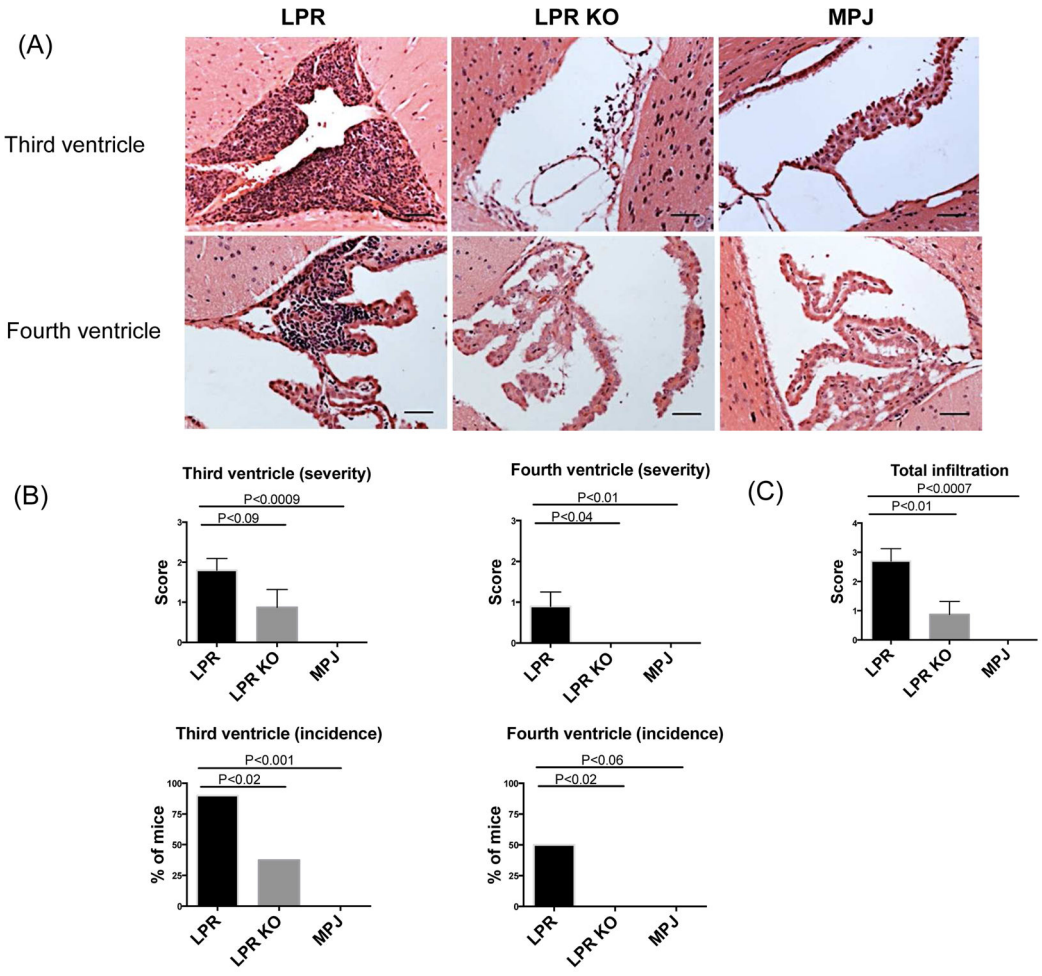

Figure 1.

Cellular infiltration in the brains of MRL/lpr Fn14WT (LPR), MRL/lpr Fn14KO (LPR KO), and MRL/MPJ (MPJ) mice. H&E staining (A) was used to assess the cellular infiltration in the third and fourth ventricles of LPR, LPR KO, and MPJ mice at 20 weeks of age. Quantification of the severity and incidence of infiltration is shown in (B). The total infiltration score of each mouse was calculated in (C). The number of mice in the LPR, LPR KO, and MPJ groups was 10, 8, and 5, respectively. The scale bars in these and all subsequent figures indicate 50 μm.

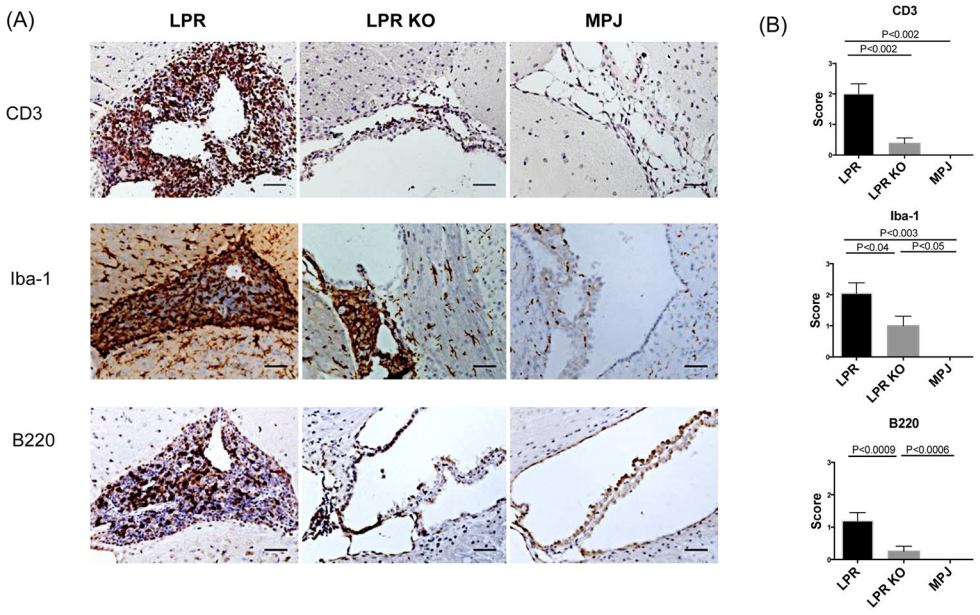

Figure 2.

T cells, macrophages, and B cells in the cellular infiltrates in the brains of LPR, LPR KO, and MPJ mice. CD3 (T cells), Iba-1 (macrophage/microglia), and B220 (B cells) staining was performed. (A) shows representative images of infiltration in the third ventricle. Staining for CD3, Iba-1, and B220 was graded (B) semi-quantatively as follows: 0=no infiltration, 1= low level of infiltration, 2=moderate level of infiltration, and 3=high level of infiltration. The number of mice in the LPR, LPR KO, and MPJ groups was 10, 8, and 5, respectively. B220 staining was done once (in duplicate) and CD3 and Iba-1 staining were repeated twice, with similar results.

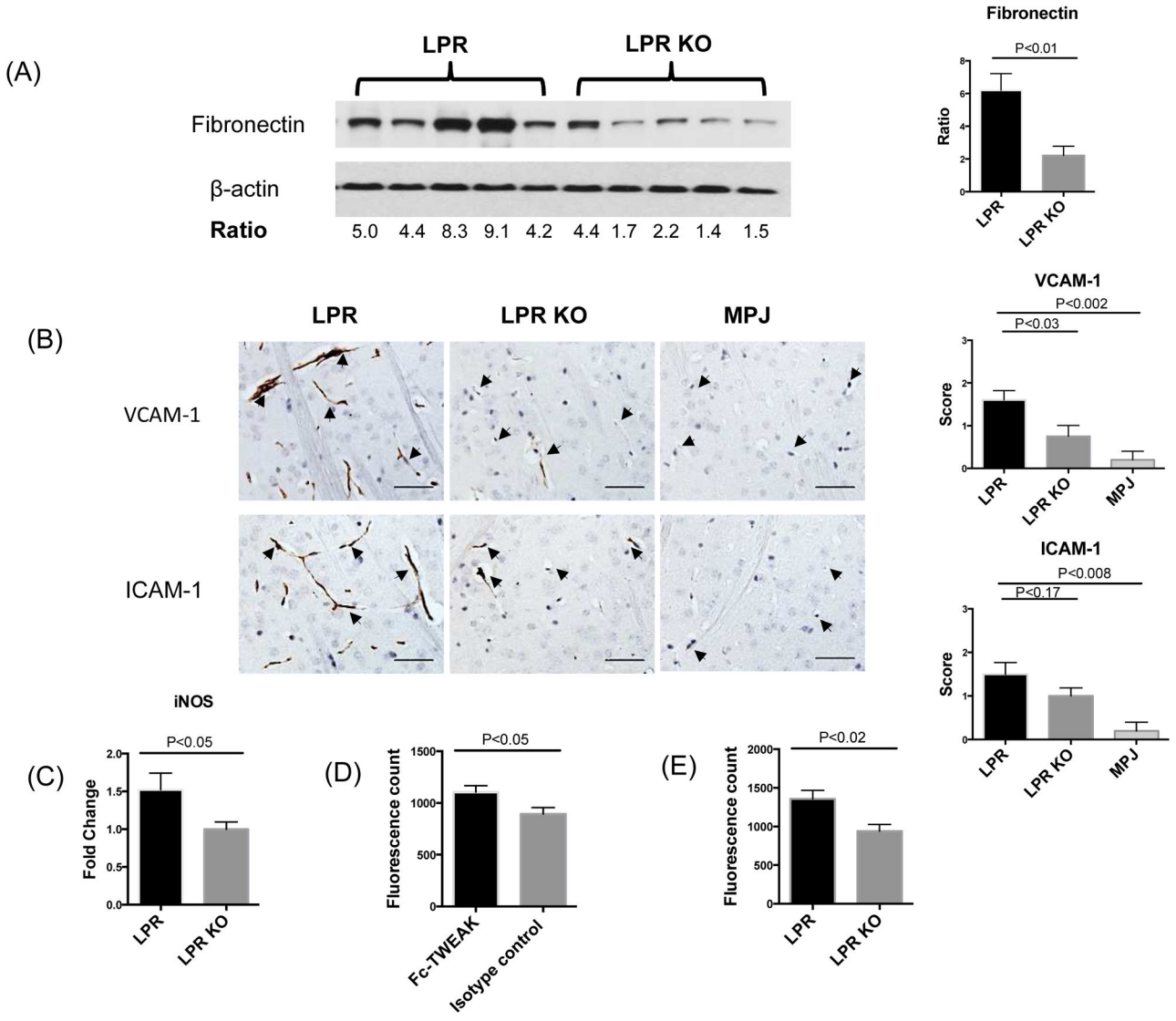

Figure 3.

BBB integrity in LPR and LPR KO mice. Western blot for fibronectin (A), left panel, was performed on brain lysates from randomly selected LPR (n=5) and LPR KO (n=5) at 20 weeks of age. Each band represents one individual mouse. Quantification of fibronectin expression by Image J is shown in (A), right panel. VCAM-1 and ICAM-1 staining is shown in (B), left panel. Arrows indicate endothelial cells. Staining intensity was graded semi-quantatively from 0 (absent staining) to 3 (maximal staining) (B), right panel. The number of mice for VCAM-1/ICAM-1 staining in the LPR, LPR KO, and MPJ groups was 10, 8, and 5, respectively. (C) iNOS was detected by qRT-PCR in cortical mRNA samples from LPR (n=8) and LPR KO (n=8) mice. The fluorescence intensity in the supernatants of brain lysates from MRL/lpr mice treated with Fc-TWEAK (n=5) or control IgG (n=5) is shown in (D). The fluorescence intensity in the supernatants of brain lysates from MRL/lpr Fn14WT (n=5) and Fn14KO mice (n=5) treated with Fc-TWEAK mice is shown in (E). Western blot for fibronectin was repeated three times, and VCAM-1/ICAM-1 staining and qPCR for

iNOS were repeated twice, with similar results. The Fc-TWEAK injection experiments were done once.

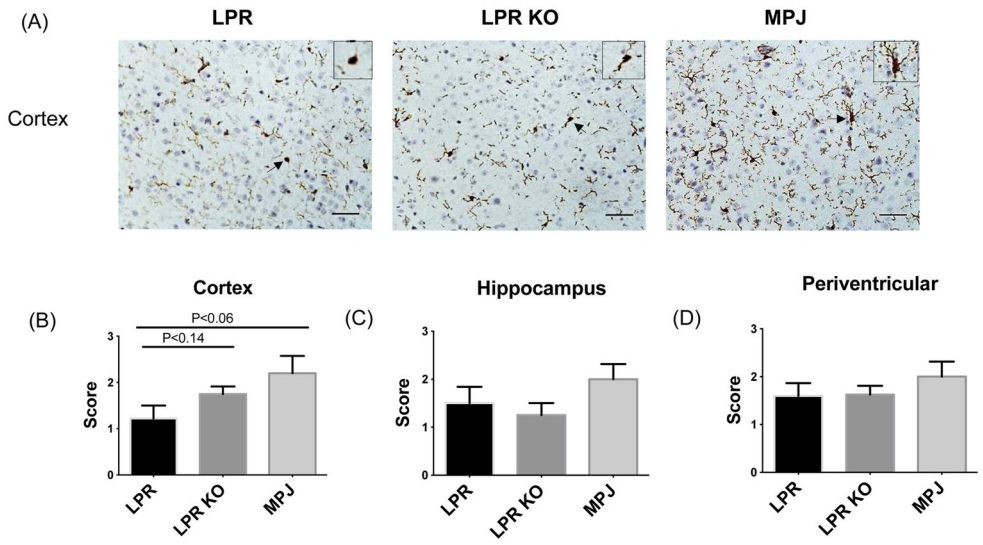

Figure 4.

Microglial activation in brains of LPR and LPR KO mice. Microglial activation was assessed by Iba-1 staining in the brain of LPR (n=10), LPR KO (n=8), and MPJ (n=5) mice at 20 weeks of age. Representative staining in the cortex is shown in (A). Arrows indicate the source location of the magnified view of microglial phenotype shown in the top right hand corner of each image. Quantification of Iba-1 staining in cortex (B), hippocampus (C), and periventricular areas (D) was graded on a scale of 0 (absent staining) to 3 (maximal staining). Iba-1 staining was repeated twice, with similar results.

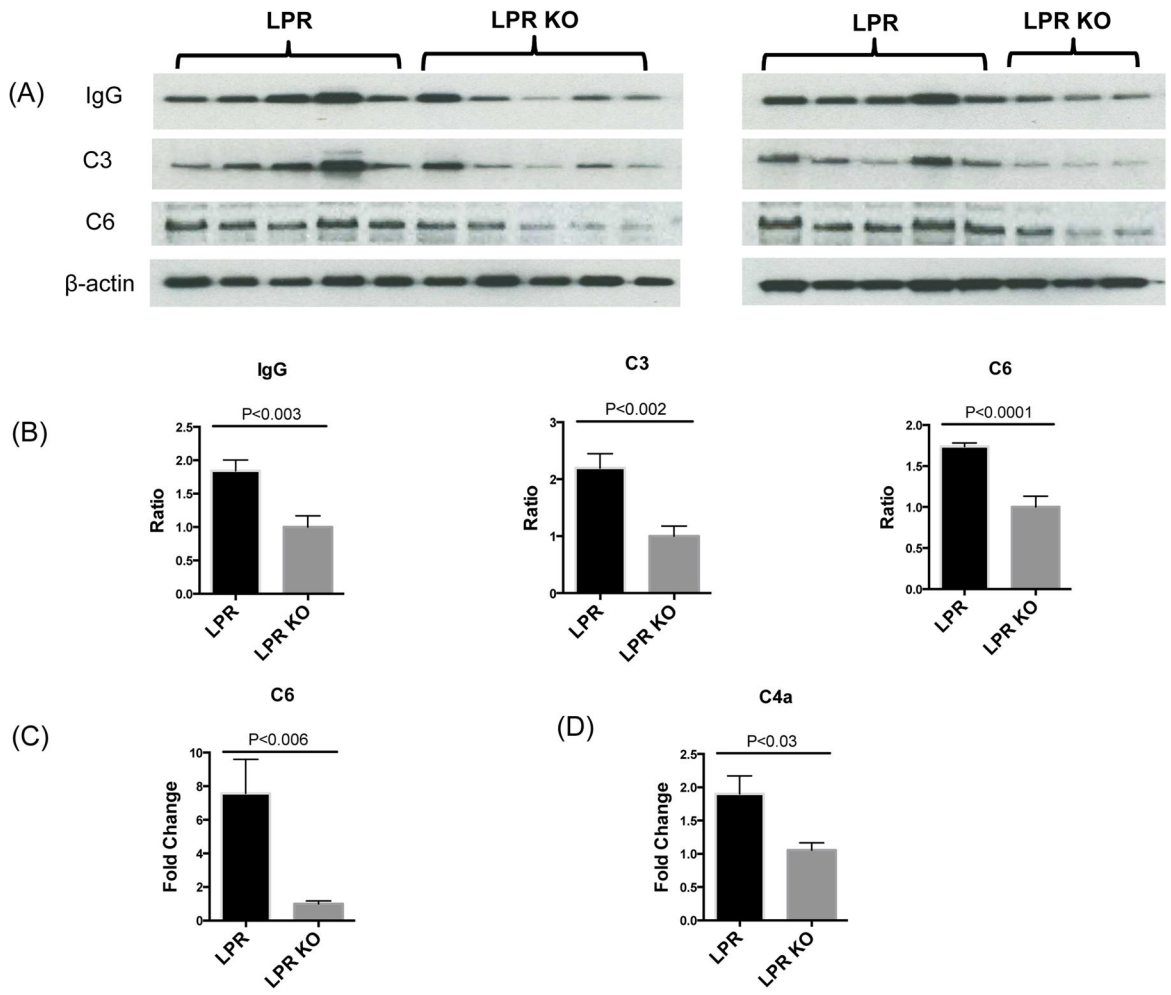

Figure 5.

Antibody and complement deposition in the brain of LPR and LPR KO mice. Brain lysates from LPR and LPR KO mice at 20 weeks of age were used to perform Western blot for IgG, C3, and C6 (A). Each band represents one individual mouse. The band intensity of IgG, C3, and C6 in each mouse was normalized to the corresponding β-actin band intensity to obtain a numerical ratio. The combined analysis of both gels is shown in (B). The average relative expression of each target protein (IgG, C3, and C6) in the LPR KO group is normalized to 1. The number of mice for Western blot for IgG, C3, and C6 in the LPR and LPR KO groups was 10 and 8, respectively. qRT-PCR was used to detect C6 (C) and C4a (D) mRNA expression in the cortex of LPR (n=8) and LPR KO (n=8) mice. Western blotting for IgG, C3, and C6, and qPCR for C6 and C4a, were repeated twice, with similar results.

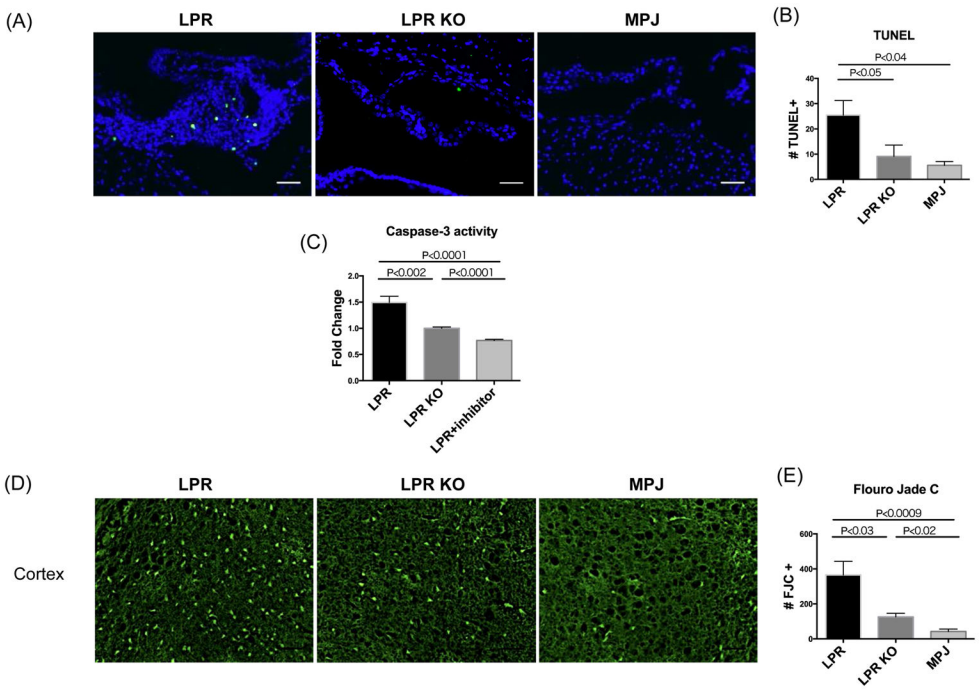

Figure 6.

Apoptosis in the brain of LPR and LPR KO mice. TUNEL staining (A) was used to evaluate apoptosis in the brains of LPR (n=10), LPR KO (n=8), and MPJ (n=5) mice at 20 weeks of age. Quantitation of the TUNEL staining is shown in (B). Caspase-3 activity assay is shown in (C). The number of mice in the assay for caspase-3 activity in the LPR, LPR KO, and LPR with inhibitor groups was 10, 9, and 10, respectively. Flouro Jade C (FJC) staining was employed to evaluate neuron degeneration in the brain of LPR (n=8), LPR KO (n=6), and MPJ (n=5) mice at 15 weeks of age. Most FJC+ positive cells are located in the cortex (D). The quantitation of cortical FJC staining is shown in (E). TUNEL staining, caspase-3 activity, and FJC staining were repeated twice, with similar results.

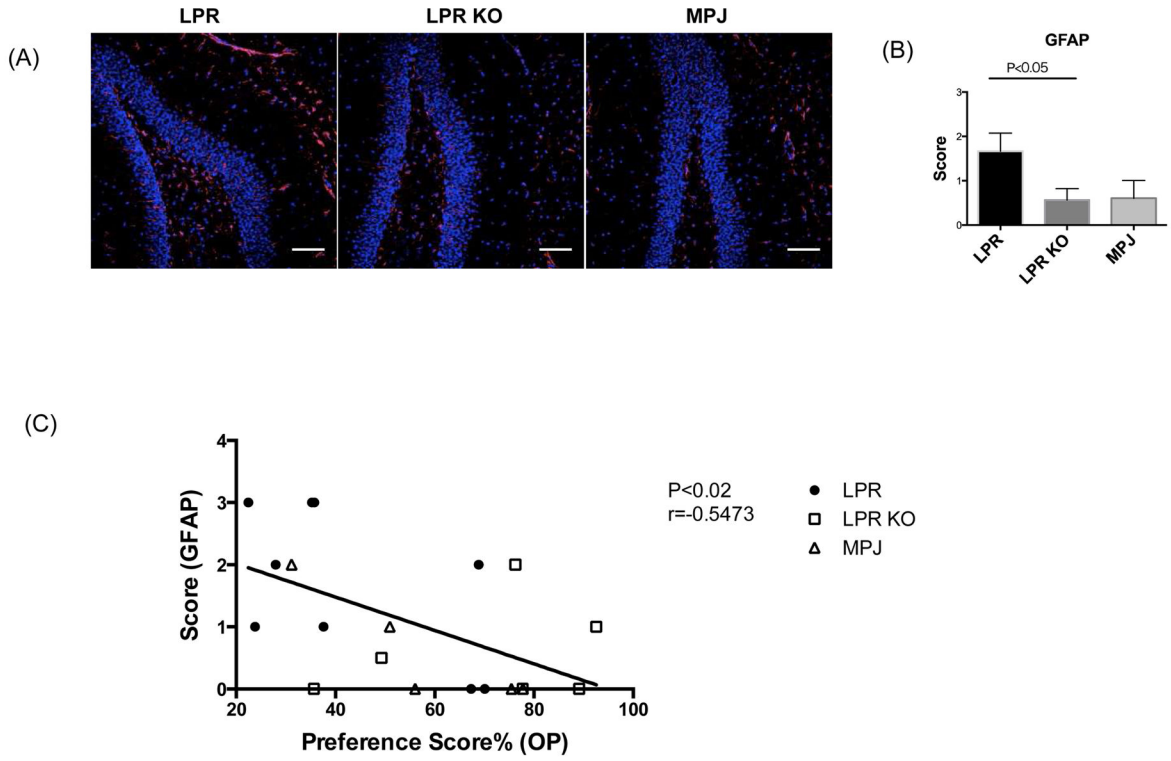

Figure 7.

Hippocampal gliosis correlates with spatial memory in LPR and LPR KO mice. GFAP staining of LPR (n=9), LPR KO (n=8), and MPJ (n=5) at 20 weeks of age is shown in (A). Representative images of each group are shown in the figure. A semi- quantitative gliosis score based on GFAP staining (B) was as follows: 0=no gliosis, 1=low level of gliosis, 2=moderate level of gliosis, and 3=high level of gliosis. GFAP staining was repeated twice, with similar results. Linear regression correlation of the scores of hippocampal gliosis with the preference scores in the object placement test is shown in (C).